

# COXETER DIAGRAMS OF 2-ELEMENTARY K3 SURFACES OF GENUS 0, AND BEYOND

VALERY ALEXEEV

ABSTRACT. We compute the Coxeter diagrams of K3 surfaces with 2-elementary Picard lattices of genus 0 and apply them to describe their (infinite) automorphism groups. We also compute several Coxeter diagrams of reflective 2-elementary hyperbolic lattices beyond the K3 case. The diagrams turn out to be remarkably symmetric, similar to the Coxeter diagrams for the unimodular lattices  $I_{1,18}$  and  $I_{1,19}$  found by Vinberg and Kaplinskaja.

## 1. INTRODUCTION

A lattice is a group  $S \simeq \mathbb{Z}^r$  together with a nondegenerate  $\mathbb{Z}$ -valued bilinear form. It is even if  $x^2$  is even for all  $x \in S$ . It is 2-elementary if  $A_S := S^*/S \simeq \mathbb{Z}_2^a$  for some  $a \geq 0$ , where  $S^* \subset S \otimes \mathbb{Q}$  is the dual group. By [Nik79] an indefinite 2-elementary lattice is uniquely determined by its signature and a triple of integers  $(r, a, \delta)$ , where  $r$  is its rank,  $a$  is the  $\mathbb{Z}_2$ -rank, and  $\delta \in \{0, 1\}$  is a certain invariant which we call coparity.

Of special interest in algebraic geometry are the hyperbolic lattices admitting a primitive embedding into the K3 lattice  $L_{K3} = H^2(K3, \mathbb{Z}) \simeq II_{3,19} = U^3 \oplus E_8^2$ . By Torelli theorem they are Picard lattices  $S_X$  of K3 surfaces. If  $S_X$  is 2-elementary then the K3 surface  $X$  admits a nonsymplectic involution. For more details we refer the reader to the papers [Nik79, Nik81]. Nikulin found a complete list of even 2-elementary K3 lattices; there are 75 of them.

An alternative to  $(r, a, \delta)$  triple of invariants is  $(g, k, \delta)$ , where  $g = 11 - \frac{1}{2}(r+a)$  is called the *genus* and  $k = \frac{1}{2}(r-a)$ . Both of these numbers are nonnegative integers that have a clear geometric meaning: if the fixed locus  $X^t$  of the involution is nonempty then it has  $k+1$  connected components and  $g$  is the sum of their genera.

The isometry group  $O(S)$  of a lattice contains two important reflections subgroups:  $W_2$  generated by reflections in  $(-2)$ -roots, and  $W_r$  generated by reflections in all roots.

The groups  $W_2$  and  $W_r$  act on the positive cone  $\mathcal{C}$ , one half of the set of positive square vectors  $\{x \in S_{\mathbb{R}} \mid x^2 \geq 0\} \subset S_X \otimes \mathbb{R}$  and on the associated hyperbolic space  $\mathcal{H} = \mathcal{C}/\mathbb{R}_{>0}$  with the fundamental polyhedra  $P_2$  and  $P_r$ . They are described by Coxeter diagrams  $\Gamma_2$ , resp.  $\Gamma_r$ , see [Vin72, Vin75]. Vinberg gave a constructive algorithm for computing the Coxeter diagram and provided sufficient conditions for its termination. In general the algorithm could be finite or infinite.

A lattice is called *2-reflective*, resp. *reflective* if  $W_2$ , resp.  $W_r$  has finite index in  $O(S)$ . This is equivalent to the condition that the polyhedron  $P_2$ , resp.  $P_r$  has finite volume, which means that the cone in the Minkowski space  $\mathbb{R}^{1,r-1}$  defined by its facets lies entirely in  $\mathcal{C}$ .

---

*Date:* September 27, 2022.

Vinberg’s theory has many applications. To begin with, the index 1 or 2 subgroup  $O^+(S)$  of  $O(S)$  that preserves the cone  $\mathcal{C}$  equals  $H \times W$  for some subgroup  $H \subset \text{Aut } \Gamma$ . Applications to K3 surfaces include:

- Automorphism groups, e.g. see [Vin83] for a famous example.
- The closure of the ample cone of a projective variety is the nef cone  $\text{Nef}(X)$  which contains important information about the geometry of  $X$ . For a K3 surface  $\text{Nef}(X)$  is identified with  $P_2$ . The rational vectors with  $v^2 = 0$  on the boundary of this cone describe elliptic pencils on  $X$ .

If the lattice  $S$  is even 2-elementary then the roots are the vectors with  $\alpha^2 = -2$  and the vectors with  $\alpha^2 = -4$  and divisibility 2. (The divisibility of a vector is defined by  $\alpha \cdot S = \text{div}(\alpha)\mathbb{Z}$ .) The polyhedron  $P_2$  is the union of the translates of  $P_r$  by the group generated by reflections in the  $(-4)$ -roots, cf. [Vin83, Prop., p.2] or [AN06, Prop. 2.4]. Thus, the groups  $W_2, W_r$  and the diagrams  $\Gamma_2, \Gamma_r$  are essentially equivalent. However, in many cases the diagram  $\Gamma_2$  is enormous, and the diagram  $\Gamma_r$  is relatively compact and manageable.

As mentioned above, there are 75 2-elementary K3 lattices. 51 of them have genus  $g \geq 2$ . For these lattices, with one easy exception, the Coxeter diagrams  $\Gamma_r$  were computed by Nikulin in [AN06, Table 1]. For the lattices on the  $g = 1$  line the diagrams  $\Gamma_r$  were computed in [AE22, Sec. 3]. The goal of the present paper is to complete the description in the remaining cases on the  $g = 0$  line.

The even 2-elementary lattices with  $g = 0$  are  $(r, a, \delta) = (10 + n, 12 - n, 1)$  for  $1 \leq n \leq 10$ ,  $(14, 8, 0)$  and  $(18, 4, 0)$ . They are all K3 lattices except for  $(14, 8, 0)$ . The case  $(11, 11, 1) = I_{1,10}(2)$  is easy and can be found e.g. in [Vin75]. The other extreme, the lattice  $(20, 2, 1)$  is far more interesting. It is the Picard lattice of one of the two “most algebraic K3 surfaces” appearing in the paper [Vin83] of Vinberg. This lattice has a unique odd extension to  $I_{1,19}$ . The Coxeter diagram  $\Gamma_r(20, 2, 1) = \Gamma_r(I_{1,19})$  was found by Vinberg and Kaplinskaja in [VK78].  $I_{1,19}$  is the largest rank unimodular hyperbolic lattice which is reflective.

We complete the remaining cases:

**Theorem 1.1.** *The 2-elementary lattices  $(17, 5, 1)$ ,  $(18, 4, 1)$  and  $(19, 3, 1)$  are not reflective. The other 2-elementary lattices on the  $g = 0$  line are reflective.*

*Proof.* In the reflective cases the proof is a computation following Vinberg’s algorithm. Each of these lattices can be written as  $U \oplus \Lambda$  or  $U(2) \oplus \Lambda$  for some root lattice  $\Lambda$ , where  $U$  is the hyperbolic plane. We choose the control vector to be a vector  $v_0$  in the first summand, with  $v_0^2 = 2$  for  $U$ , resp.  $v_0^2 = 4$  for  $U(2)$ , and run the algorithm using a custom Sage [Sag22] script written for this purpose.

We checked the completeness of the diagrams directly, by confirming that the cones in the Minkowski spaces  $\mathbb{R}^{1,r-1}$  defined by the roots of  $\Gamma_r$  lie entirely in  $\bar{\mathcal{C}}$ .

For the diagrams without broken edges the easy sufficient condition of [Vin75] also works to verify the completeness by hands: the diagrams do not contain Lannér subgraphs, and every connected parabolic subdiagram is contained in a maximal parabolic subdiagram of maximal rank. For the diagrams with broken edges, the criterion of [Vin72, Prop. 2] works.

For the nonreflective lattices the proof is as follows. One has

$$(19, 3, 1) = A_1 \oplus (18, 2, 1) \text{ and } (18, 4, 1) = A_1 \oplus (17, 3, 1), \text{ where } A_1 = \langle -2 \rangle.$$

The polyhedron  $P_r(18, 2, 1)$  is a face of  $P_r(19, 3, 1)$  and  $\Gamma_r(18, 2, 1)$  is smaller than  $\Gamma_r(19, 3, 1)$ , see [AE22, Lem. 4.14]. Similarly for  $(18, 4, 1)$ . The diagrams  $\Gamma_r(18, 2, 1)$ ,  $\Gamma_r(17, 3, 1)$  are infinite by [AE22, Thm. 3.6], and so are  $\Gamma_r(19, 3, 1)$  and  $\Gamma_r(18, 4, 1)$ .

Finally, one has  $(17, 5, 1) \simeq U(2) \oplus \Lambda$  for any even 2-elementary negative definite lattice  $\Lambda$  with  $(r, a, \delta) = (15, 3, 1)$ , where  $U$  is a hyperbolic plane. If the lattice  $(17, 5, 1)$  were reflective then  $\Lambda$  would correspond to a maximal parabolic subdiagram of  $\Gamma_r$  and the root sublattice  $R(\Lambda)$  would have rank equal to  $r(\Lambda) = 15$ . But by [AE22, Table 2] there exists  $\Lambda$  with  $R(\Lambda) = A_{13}A_1(2)$  of rank 14.  $\square$

The diagrams for  $(11, 11, 1)$ ,  $(12, 10, 1)$ ,  $(13, 9, 1)$ ,  $(14, 8, 0)$  and  $(14, 8, 1)$  are relatively small and we give them in Figure 2. The others are too large to draw directly. However, it turns out that they are remarkably symmetric and can be described in a way similar to the papers [VK78, Vin83] of Vinberg and Kaplinskaja.

**Definition 1.2.** Let  $G$  be a graph and  $n \geq 2$  be an integer. Define the edge  $n$ -fold graph  $G^{(n)}$  by subdividing each edge of  $G$  into  $n$  edges and inserting  $n - 1$  intermediate vertices. Thus,  $G^{(n)}$  has  $n|E_G|$  edges and  $|V_G| + (n - 1)|E_G|$  vertices.

**Definition 1.3.** We say that a diagram  $\Gamma$  is built on top of a simple graph  $H$  if it contains a subdiagram of the main roots isomorphic to  $H$ , and the additional roots are defined in terms of the main roots by some specified rules.

For the 2-elementary lattices of this paper the main roots are the  $(-2)$ -roots of divisibility 1. For the lattices in Theorem 1.4 the following is also true: if a main root  $\alpha$  and an additional root  $\beta$  are connected then  $\alpha\beta = 2$ .

By [VK78] the Coxeter diagrams of  $I_{1,18}$  and  $I_{1,19}$  are built on top of  $K_4^{(4)}$  and  $G^{(2)}$  for the Petersen graph  $G$ . Also, the Coxeter diagram of the Picard lattice of the second “most algebraic K3 surface”  $X_3$  in [Vin83] is built on top of  $K_{3,3}^{(3)}$ .

**Theorem 1.4.** For  $n = 3, 4, 5, 6$  the Coxeter diagram  $\Gamma_r$  of the even 2-elementary lattice  $(10 + n, 12 - n, 1)$  is built on top of  $G^{(2)}$ , where  $G = K_n$  is the complete graph on  $n$  vertices. The diagram  $\Gamma_r$  for  $(18, 4, 0)$  is built on top of  $G^{(2)}$ , where  $G = K_{4,4}$  is the complete bipartite graph on 8 vertices, and that of  $(14, 8, 0)$  on top of  $G^{(2)}$  for  $G = D_4$ . In all cases one has  $\text{Aut } \Gamma_r = \text{Aut } G$  and  $O^+(S) = \text{Aut } G \times W_r$ .

*Proof.* The proof is by observation, analyzing the structure of the diagrams obtained in Theorem 1.1. The claim about  $O^+(S)$  follows because the roots generate the lattice.  $\square$

In the course of describing the diagrams we also give a presentation of the lattices that make the  $\text{Aut } G$  group action on it explicit. Once this structure is revealed, in most cases it becomes obvious that there is a nice choice of an  $(\text{Aut } G)$ -symmetric control vector for which Vinberg’s algorithm terminates in just a couple of steps and can be done entirely by hands.

I have also computed a few interesting diagrams for the even 2-elementary lattices beyond the K3 lattices. The following theorem is proved by the same methods. For a graph  $H$ ,  $L(H)$  denotes its line graph, a.k.a. the edge graph.

**Theorem 1.5.** The Coxeter diagram of  $(15, 9, 1)$  is built on top of the bipartite complement of the Heawood graph, with  $\text{Aut } G \simeq \text{PSL}(2, 7)$ . The Coxeter diagram of  $(15, 11, 1)$  is built on top of  $G = L(K_{3,3})$ , and the diagram of  $(16, 12, 1)$  on top of  $G = L(K_6)$ . In all cases one has  $\text{Aut } \Gamma_r = \text{Aut } G$  and  $O^+(S) = \text{Aut } G \times W_r$ .

The lattices  $(r, r, 1) = I_{1,r-1}(2)$  for  $r \leq 20$  are reflective by [Vin75, VK78]. Other even 2-elementary reflective lattices, all with small automorphism groups, include  $(14, 12, 0)$ ,  $(14, 12, 1)$ ,  $(15, 13, 1)$ ,  $(16, 14, 1)$ .

It is interesting to compare the diagrams of the present paper with the diagrams on the  $g = 1$  line, computed in [AE22, Sec. 3]. The latter are smaller but less symmetric: they have the dihedral symmetry of  $n$ -gons. Most diagrams for  $g \geq 2$  do not have any symmetries at all. However, by [AE22, Lem. 4.14] the diagram  $\Gamma_r(r, a, \delta)$  of genus  $g$  can be obtained from the diagram  $\Gamma'_r(r+1, a+1, 1)$  of genus  $g-1$  by a simple rule.  $\text{Aut } \Gamma_r$  is the stabilizer in  $\text{Aut } \Gamma'_r$  of a  $(-2)$ -root of divisibility 2.

The  $g = 1$  diagrams turn out to be the key to understanding degenerations of K3 surfaces with a nonsymplectic involution via a mirror symmetry construction. The lattices with  $g \leq 0$  do not appear as targets of the mirror symmetry correspondence of the ordinary K3 surfaces. But they may appear on the mirrors of higher-dimensional hyperkähler varieties. What do the symmetries of the Coxeter diagrams imply about their degenerations?

In Section 2 we fix the notation for the lattices and diagrams. In Section 3 we give the Coxeter diagrams and list maximal parabolic subdiagrams. In Section 4 we apply the Coxeter diagrams of the K3 lattices that we found to describe the automorphism groups of the corresponding K3 surfaces. They are all infinite.

**Acknowledgements.** I would like to thank Boris Alexeev for help with computations at critical junctures. I was partially supported by the NSF grant DMS-2201222.

## 2. NOTATION

Because we are coming from the algebraic geometry direction, for us a hyperbolic lattice of rank  $r$  has signature  $(1, r-1)$ .  $A_n, D_n, E_n$  are the standard root lattices generated by  $(-2)$ -roots, and they are *negative definite*.  $U = \begin{pmatrix} 0 & 1 \\ 1 & 0 \end{pmatrix}$  denotes the hyperbolic plane. For any lattice  $H$ ,  $H(n)$  is the same group with the product  $(x, y)_{H(n)} = n(x, y)_H$ . For the 2-elementary lattices with short  $(-2)$  and long  $(-4)$ -roots additionally there are root lattices  $B_n(2), C_n$  and  $F_4$ . Considered as the  $(-2)$ -root lattices they are  $A_1^n, D_n$ , and  $D_4$  respectively.

We refer to [Vin72] for Vinberg's theory. We use the notations of that paper for elliptic and parabolic Coxeter diagrams. The vertices of  $\Gamma_r$  denote the roots  $\alpha_i$  orthogonal to the facets of  $P_r$ . The types of edges specify the angle  $\theta$  between  $\alpha_i, \alpha_j$ . A single line means  $\theta = \pi/3$ , double line  $\theta = \pi/4$ , no line  $\theta = \pi/2$ , a bold line means that the hyperplanes defining the two facets meet at an infinite point of the hyperbolic space  $\mathcal{H}$ , and a broken line means that they are skew.

For a 2-elementary lattice, we denote the short,  $(-2)$ -roots by white vertices and the long,  $(-4)$ -roots by black vertices. Then the types of edges correspond to the following intersection numbers  $\alpha_i \cdot \alpha_j$  between the roots:

$\alpha_i^2$	$\alpha_j^2$	simple	double	bold	broken
-2	-2	1		2	$> 2$
-4	-4	2		4	$> 4$
-2	-4		2		$> 2$

The parabolic  $\tilde{A}_n, \tilde{D}_n, \tilde{E}_n$  diagrams could consist either of all short, or of all long roots. If this parabolic subdiagram  $\Gamma \subset \Gamma_r$  corresponds to a vector  $v \in S$  with  $v^2 = 0$  then its image in  $v^\perp/v$  spans a 2-elementary root system. For all white vertices it is  $A_n, D_n, E_n$ , and for all black vertices it is  $A_n(2), D_n(2), E_n(2)$ .

Similarly, for  $\tilde{B}_n, \tilde{C}_n$  and  $\tilde{F}_4$  there are two versions, *short* and *long*, which are dominated by the short, resp. long roots. We list them in Figure 1. Note that “dominated” means “for large  $n$ ”. For example for  $\tilde{C}_n$  the short roots start to dominate only for  $n \geq 4$ . One should keep in mind that  $D_2 = A_1^2$  and  $D_3 = A_3$ .

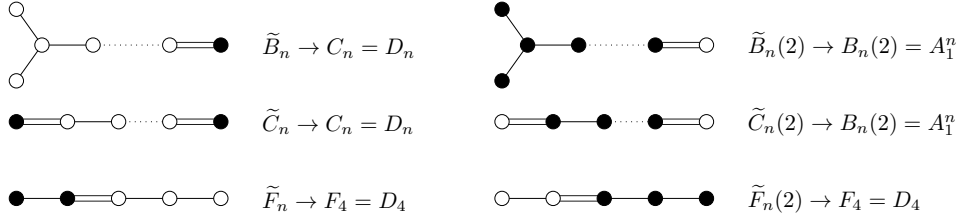


FIGURE 1. Extended Dynkin diagrams dominated by short or long vectors

By [AE22, Prop. 5.5] the isotropic vectors  $v \in S$ ,  $v^2 = 0$  are of three types. Denoting  $\bar{S} = v^\perp/v$  and with  $v$  a vector in the first summand, the types are:

- (1) (odd)  $S = U \oplus \bar{S}$ ,  $a_{\bar{S}} = a_S$ ,  $\delta_{\bar{S}} = \delta_S$ .
- (2) (even ordinary)  $S = U(2) \oplus \bar{S}$ ,  $a_{\bar{S}} = a_S - 2$ ,  $\delta_{\bar{S}} = \delta_S$ .
- (3) (even characteristic)  $S = I_{1,1}(2) \oplus \bar{S}$ ,  $a_{\bar{S}} = a_S - 2$ ,  $\delta_S = 1$  and  $\delta_{\bar{S}} = 0$ .

### 3. COXETER DIAGRAMS

We give the diagrams for the lattices  $(11, 11, 1)$ ,  $(12, 10, 1)$ ,  $(13, 9, 1)$ ,  $(14, 8, 0)$  and  $(14, 8, 1)$  in Figure 2.

3A. **(11, 11, 1)**. This lattice is isomorphic to

$$U(2) \oplus E_8(2) \oplus A_1 = I_{1,10}(2)$$

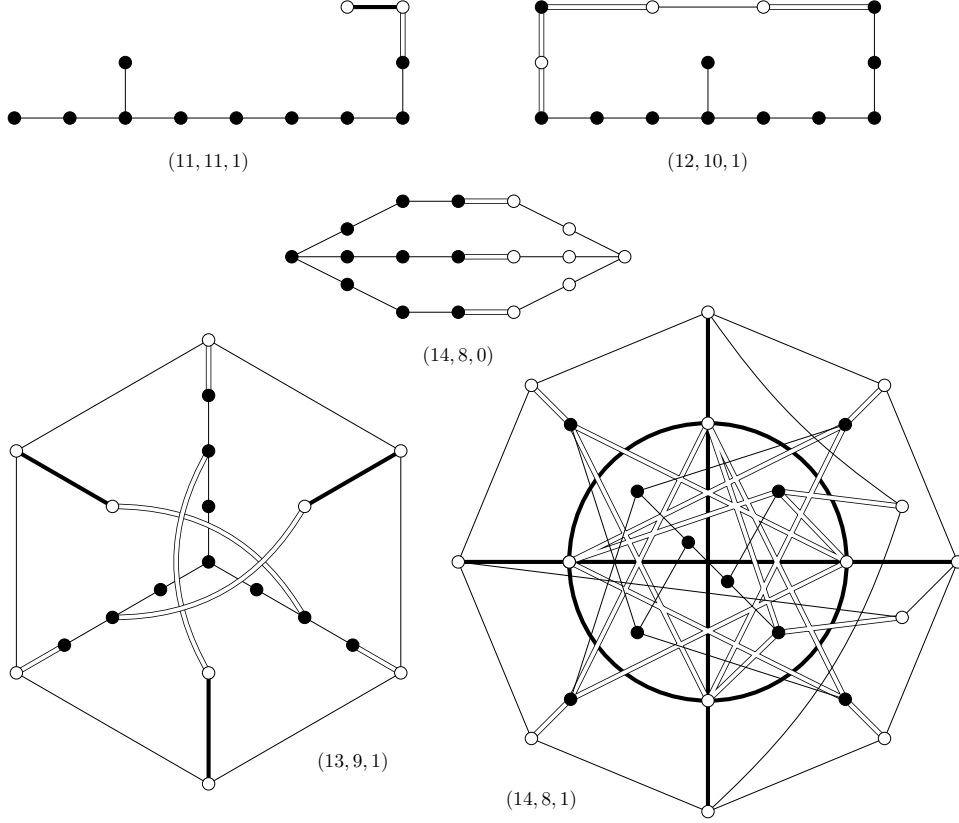
The Coxeter diagram  $\Gamma_r$  has 12 roots. There are two isotropic vectors  $v$  modulo  $O^+(S)$ . They correspond to the following subdiagrams of the Coxeter diagram, both even ordinary:  $\tilde{E}_8(2)\tilde{A}_1$  and  $\tilde{B}_9(2)$ . The automorphism group of  $\Gamma_r$  is trivial.

3B. **(12, 10, 1)**. This lattice is isomorphic to

$$U \oplus E_8(2) \oplus B_2(2).$$

The Coxeter diagram has 14 roots. Note that for the parabolic subdiagram  $\tilde{C}_3$  the corresponding root lattice  $v^\perp/v$  is  $C_3 = D_3 = A_3$ . There are 5 maximal parabolic subdiagrams listed below. The automorphism group of  $\Gamma_r$  is trivial.

- (1) odd:  $\tilde{E}_8(2)\tilde{C}_2(2), \tilde{C}_{10}(2)$ .
- (2) even ordinary:  $\tilde{E}_7(2)\tilde{C}_3, \tilde{B}_6(2)\tilde{F}_4(2), \tilde{B}_8(2)\tilde{C}_2$ .

FIGURE 2. Coxeter diagrams  $\Gamma_r$  for ranks  $r \leq 14$ 

3C. **(13, 9, 1)**. This lattice is isomorphic to

$$U \oplus F_4 \oplus B_7(2) = U \oplus D_4 \oplus A_1^7.$$

when considered as a root lattice for the  $(-2)$  and  $(-4)$ -roots, or for the  $(-2)$ -roots only, respectively. The Coxeter diagram has 19 roots. There are 22 maximal parabolic subdiagrams, and 7 modulo  $\text{Aut } \Gamma_r = S_2$ :

- (1) odd:  $\tilde{C}_8(2)\tilde{C}_3(2)$ ,  $\tilde{E}_7(2)\tilde{B}_3\tilde{A}_1$ ,  $\tilde{C}_7(2)\tilde{F}_4$ .
- (2) even ordinary:  $\tilde{F}_4^2(2)\tilde{B}_3(2)$ ,  $\tilde{C}_6\tilde{B}_5(2)$ ,  $\tilde{B}_6(2)\tilde{C}_4\tilde{A}_1$ ,  $\tilde{E}_6(2)\tilde{A}_5$ .

It is clear that this diagram is built on top of the graph  $K_3^{(2)}$ . The main roots are the 6 roots on the outside hexagon, and the additional roots come in four layers culminating with the central vertex. The roots generate the lattice, so the  $S_3$ -action on  $\Gamma_r$  extends to the action on the lattice  $H$  itself.

3D. **(14, 8, 0)**. This lattice is isomorphic to

$$U(2) \oplus F_4^3 = U(2) \oplus D_4^3.$$

The Coxeter diagram has 17 roots. There are 11 maximal parabolic subdiagrams, and 5 modulo  $\text{Aut } \Gamma_r = S_3$ :

- (1) odd:  $\tilde{E}_7(2)\tilde{B}_5, \tilde{C}_8(2)\tilde{F}_4$ .
- (2) even ordinary:  $\tilde{F}_4^3(2), \tilde{C}_6\tilde{B}_6(2), \tilde{E}_6\tilde{E}_6(2)$ .

It is clear that this diagram is built on top of the graph  $D_4^{(2)}$ , where  $D_4$  is a tree with four vertices, the central vertex of degree 3 and three ends.

3E. **(14, 8, 1)**. This lattice is isomorphic to

$$U \oplus F_4^2 \oplus B_4(2) = U \oplus D_4^2 \oplus A_1^4.$$

For the choice of the control vector  $v_0 \in U$  with  $v_0^2 = 2$ , Vinberg's algorithm ends in 17 steps. The Coxeter diagram has 24 roots. There are 127 maximal parabolic subdiagrams, and 15 modulo  $\text{Aut } \Gamma_r = S_4$ :

- (1) odd:  $\tilde{F}_4^2\tilde{C}_4(2), \tilde{D}_6\tilde{C}_6(2), \tilde{C}_6(2)\tilde{B}_4\tilde{C}_2(2), \tilde{E}_6(2)\tilde{A}_5\tilde{A}_1, \tilde{D}_6(2)\tilde{B}_3^2, \tilde{C}_4^3(2)$ .
- (2) even ord:  $\tilde{C}_6\tilde{F}_4(2)\tilde{C}_2, \tilde{C}_4^2\tilde{B}_4(2), \tilde{D}_6\tilde{B}_5(2)\tilde{A}_1, \tilde{E}_7\tilde{B}_5(2), \tilde{C}_8\tilde{B}_4(2), \tilde{A}_7\tilde{D}_5(2)$ .
- (3) even char:  $\tilde{F}_4^3(2), \tilde{C}_6\tilde{B}_6(2), \tilde{E}_6\tilde{E}_6(2)$ .

It is clear that this diagram is built on top of the graph  $K_4^{(2)}$ . Denote the main roots  $\alpha_i^m$  with  $i = 1, 2, 3, 4$  for the 4 vertices and  $\alpha_{ij}^m$  with  $1 \leq i < j \leq 4$  for the 6 edges of  $K_4$ . For each edge there is an additional  $(-2)$ -root  $\alpha_{ij}$  attached to it, and a  $(-4)$ -root  $\alpha_{ij}^+$  attached to  $\alpha_{ij}$ . One has  $\alpha_{ij}^m\alpha_{ij} = \alpha_{ij}\alpha_{ij}^+ = 2, \alpha_{ij}^m\alpha_{ij}^+ = 0$ . Let  $\bar{\alpha}_{ij} = \alpha_{ij} + \alpha_{ij}^+$ .

Then the 12 roots  $\alpha_{ij}, \bar{\alpha}_{ij}$  are mutually orthogonal, and are also orthogonal to the central  $(-4)$ -root  $\alpha_{cen}$ . The orthogonal complement of these 13 vectors in  $H$  is  $\mathbb{Z}h$  with  $h = \frac{1}{2}(\sum \alpha_i^m + \sum \alpha_{ij} + \sum \bar{\alpha}_{ij})$ . One has  $h^2 = 4$ . Set  $e = \frac{1}{2}(h + \alpha_{cen})$  and  $f = \frac{1}{2}(h - \alpha_{cen})$ . Then the 14 vectors  $\alpha_{ij}, \bar{\alpha}_{ij}, e, f$  form the standard basis of a sublattice of  $H$  isomorphic to  $(I_{0,12} \oplus U)(2)$ . Thus,  $H$  can be identified with an  $S_4$ -invariant lattice lying between it and its dual  $(I_{0,12} \oplus U)(\frac{1}{2})$ .

Picking  $v_0 = h$  to be the control vector, Vinberg's algorithm ends in two steps.

3F. **(15, 7, 1)**. This lattice is isomorphic to

$$U \oplus F_4^3 \oplus A_1 = U \oplus D_4^3 \oplus A_1.$$

The Coxeter diagram contains 60 roots. As in Definition 1.3, it is build on top of the graph  $K_5^{(2)}$ . The subdiagram of the main roots is  $K_5^{(2)}$ , as shown on the left in Fig. 3. The 15 main roots form a basis of the lattice.

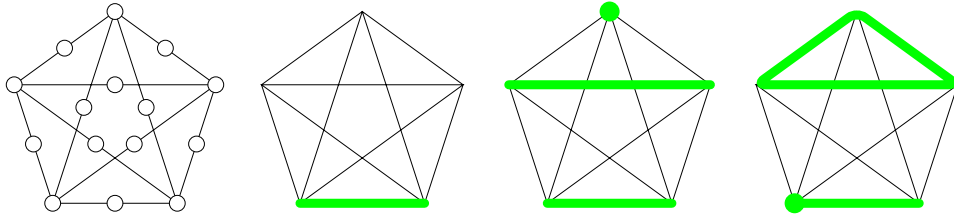


FIGURE 3. Additional roots for (15, 7, 1)

The additional roots  $\alpha_C$  correspond to the following collections of vertices and edges of the graph  $G = K_5$ , pictured in Fig. 3:

- (1) 10  $(-4)$ -roots with  $C$  an edge, e.g.  $C = \{12\}$ .

- (2) 15  $(-2)$ -roots with  $C$  a vertex and two edges, all disjoint from each other, e.g.  $C = \{1, 23, 45\}$ .
- (3) 20  $(-2)$ -roots with  $C = \{1, 12, 34, 35, 45\}$  etc, with  $C$  consisting of three edges in a triangle, an edge disjoint from it, plus a vertex on the latter edge.

We can specify the collections  $C$  by marking some vertices of the subdiagram  $G^{(2)}$  of the main roots. Equivalently, and easier to picture, we can specify them by marking some vertices and edges of the initial graph  $G = K_5$ . We will do the latter, and use this presentation of the additional roots for the bigger graphs below as well.

The edges between the main and additional roots are specified in Definition 1.3. We now list the typical edges between the additional roots  $\alpha_C, \alpha_{C'}$ . The others follow by  $S_5$ -symmetry.

- (1)  $\alpha_{12}$  is connected by a single line to  $\alpha_{34}$ ; by a double line to  $\alpha_{3,14,25}$ ; and by a broken line to  $\alpha_{3,13,24,25,45}$ .
- (2)  $\alpha_{1,23,45}$  is connected by a double line to  $\alpha_{24}$ ; a bold line to  $\alpha_{1,24,35}, \alpha_{2,13,45}, \alpha_{1,12,34,35,45}$  and  $\alpha_{2,14,15,23,45}$ ; and a broken line to  $\alpha_{2,14,35}, \alpha_{2,12,34,35,45}$  and  $\alpha_{2,13,14,25,34}$ .
- (3)  $\alpha_{1,12,34,35,45}$  a bold line to  $\alpha_{1,23,45}$  and  $\alpha_{3,12,45}$ ; and a broken line to  $\alpha_{23}, \alpha_{2,13,45}, \alpha_{3,14,25}, \alpha_{1,13,24,25,45}, \alpha_{2,12,34,35,45}, \alpha_{3,12,15,25,34}, \alpha_{3,14,15,23,45}, \alpha_{2,14,15,23,45}$ , and  $\alpha_{3,13,24,25,45}$ .

The entire intersection matrix can be easily described as follows. The main roots  $\alpha_1^m, \alpha_{12}^m$  etc. form a basis of the lattice  $S$ . Let  $\omega_1$  and  $\omega_{12}$  etc. denote the vectors such that  $\alpha_I^m \omega_J = 2\delta_{IJ}$ , i.e. forming twice the dual basis. Then  $\alpha_C = \sum_{I \in C} \omega_I$ , where  $I$  is one of the sets  $1, \dots, 5, 12, \dots, 45$ . Thus, it suffices to specify the typical intersection numbers between  $\omega_I$ . They are:

$$\omega_1^2 = -6, \quad \omega_1 \omega_2 = 2, \quad \omega_1 \omega_{12} = -2, \quad \omega_1 \omega_{23} = 2, \quad \omega_{12}^2 = -4, \quad \omega_{12} \omega_{23} = 0, \quad \omega_{12} \omega_{34} = 2.$$

The  $(-4)$ -vectors of  $\Gamma_r$  form the Petersen graph on 10 vertices, with simple edges.

There are 1027 maximal parabolic subdiagrams, and 20 modulo  $\text{Aut } \Gamma_r = S_5$ :

- (1) odd:  $\tilde{E}_7 \tilde{C}_6(2), \tilde{B}_6 \tilde{F}_4 \tilde{C}_3(2), \tilde{B}_6 \tilde{C}_6(2) \tilde{A}_1, \tilde{D}_6 \tilde{C}_5(2) \tilde{C}_2(2), \tilde{B}_8 \tilde{C}_5(2), \tilde{A}_5 \tilde{A}_5(2) \tilde{B}_3, \tilde{F}_4^3 \tilde{A}_1, \tilde{C}_4(2) \tilde{B}_4^2 \tilde{A}_1, \tilde{C}_{10} \tilde{B}_3(2), \tilde{E}_6 \tilde{E}_6(2) \tilde{A}_1, \tilde{A}_7 \tilde{D}_5(2) \tilde{A}_1, \tilde{D}_4 \tilde{C}_3^3(2)$ .
- (2) even ordinary:  $\tilde{E}_7 \tilde{B}_5(2) \tilde{A}_1, \tilde{D}_8 \tilde{B}_4(2) \tilde{A}_1, \tilde{E}_8 \tilde{B}_5(2), \tilde{C}_8 \tilde{F}_4(2) \tilde{A}_1, \tilde{E}_7 \tilde{F}_4(2) \tilde{C}_2, \tilde{D}_6 \tilde{C}_4 \tilde{B}_3(2), \tilde{A}_9 \tilde{A}_4(2), \tilde{C}_6^2 \tilde{A}_1$ .

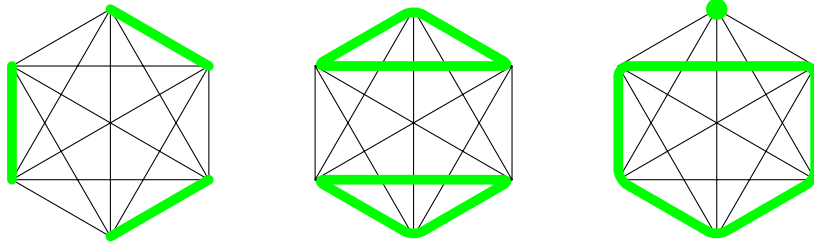
3G. **(16, 6, 1)**. This lattice is isomorphic to

$$U(2) \oplus C_8 \oplus C_6 = U(2) \oplus D_8 \oplus D_6.$$

The Coxeter diagram contains 118 roots. The starting graph  $G$  is  $K_6$ , a complete graph on 6 vertices. As in Definition 1.3, the subdiagram of the main roots is  $K_6^{(2)}$ . It has 6  $(-2)$ -roots corresponding to vertices of  $K_6$ —call them 1, 2, 3, 4, 5, 6—and 15  $(-2)$ -roots corresponding to the edges of  $K_6$ —call them 12, 13 etc, for a total of 21 main roots. Let us denote the main roots  $\alpha_1^m, \alpha_{12}^m$  etc.

The additional roots  $\alpha_C$  correspond to the following collections of vertices and edges of the starting graph  $G$ , pictured in Fig. 4, modulo  $S_6$ :

- (1) 15  $(-4)$ -roots  $\alpha_{12,34,56}$  for  $C$  equal to a triple of disjoint edges.
- (2) 10  $(-4)$ -roots  $\alpha_{12,23,31,45,56,64}$  for  $C$  equal to the 6 edges in two disjoint triangles.
- (3) 72  $(-2)$ -roots  $\alpha_{12,23,34,45,51,6}$  for a cycle of 5 edges and a vertex.

FIGURE 4. Additional roots for  $(16, 6, 1)$ 

The 15 main roots  $\alpha_{12}$  for the edges, together with  $\alpha^m = \alpha_1^m + \alpha_2^m + \cdots + \alpha_6^m$  span the lattice over  $\mathbb{Q}$ . Let  $\omega_{12}, \dots, \omega_{56}, \omega$  be twice the dual basis. Then the additional roots are  $\alpha_C = \sum_{I \in C} \omega_I$ , where we formally set  $\omega_1 = \omega$  etc for the vertices. The multiplication table for this dual basis is very easy:  $\omega_{12}^2 = -\frac{16}{9}$  for the edges, and all the other products and squares are  $\frac{2}{9}$ . Thus,

$$\omega_C \cdot \omega_{C'} = \frac{2}{9} |C| \cdot |C'| - 2 |C \cap C' \cap \text{Edges}(G)|.$$

Explicitly, the edges between the additional roots are:

- (1) Two roots of type (1) are joined by a bold line if they don't share an edge.
- (2) Two roots of type (2) are joined by a bold line.
- (3) Two roots of type (3) are joined by a bold line if they share 3 edges, and by a broken line otherwise.
- (4) Roots of types (1) and (2) are joined by a bold line if they don't share an edge, by a single line if they share one edge.
- (5) Roots of types (1) and (3) are joined by a broken line if they don't share edges, and by a double line if they share one edge.
- (6) Roots of types (2) and (3) are joined by a double line if they share three edges, and by a broken line if they share fewer edges.

The 15 additional roots  $\alpha_{12}$  etc. for the edges are mutually orthogonal  $(-2)$ -roots. Denote by  $v = \alpha_1^m + \cdots + \alpha_6^m$  the sum of the main roots for the vertices of  $K_6$  and by  $e = \alpha_{12}^m + \cdots + \alpha_{56}^m$  the sum of the main roots for the edges of  $K_6$ . Then  $h = \frac{1}{3}(v+e)$  is a vector in  $H$  satisfying  $h^2 = 2$  and orthogonal to the above 15 roots. Then  $h, \alpha_{12}, \dots, \alpha_{56}$  form a sublattice of  $H$  isomorphic to  $I_{1,15}(2)$ . Thus,  $H$  can be identified with an  $S_6$ -symmetric lattice lying between it and its dual  $I_{1,15}(\frac{1}{2})$ .

With the control vector  $v_0 = h$ , Vinberg's algorithms terminates in four steps.

There are 8917 maximal parabolic subdiagrams, 28 modulo  $\text{Aut } \Gamma_r = S_6$ :

- (1) odd:  $\tilde{B}_6 \tilde{C}_4(2) \tilde{B}_4, \tilde{B}_{10} \tilde{C}_4(2), \tilde{B}_6^2 \tilde{C}_2(2), \tilde{E}_8 \tilde{C}_6(2), \tilde{D}_6 \tilde{B}_4 \tilde{C}_3(2) \tilde{A}_1, \tilde{D}_8 \tilde{C}_4(2) \tilde{C}_2(2), \tilde{E}_6 \tilde{A}_5(2) \tilde{B}_3, \tilde{B}_8 \tilde{F}_4 \tilde{C}_2(2), \tilde{B}_8 \tilde{C}_6(2), \tilde{B}_6 \tilde{F}_4^2, \tilde{E}_7 \tilde{F}_4 \tilde{C}_3(2), \tilde{E}_7 \tilde{C}_5(2) \tilde{C}_2(2), \tilde{D}_6 \tilde{C}_3^2(2) \tilde{C}_2(2), \tilde{D}_4^2 \tilde{C}_2^3(2), \tilde{A}_5^2 \tilde{A}_2^2(2), \tilde{A}_7 \tilde{A}_3(2) \tilde{B}_3 \tilde{A}_1(2), \tilde{B}_4^2 \tilde{C}_2(2), \tilde{A}_9 \tilde{A}_4(2) \tilde{A}_1.$
- (2) even ordinary:  $\tilde{E}_8 \tilde{F}_4(2) \tilde{C}_2, \tilde{D}_{10} \tilde{B}_3(2) \tilde{A}_1, \tilde{C}_{10} \tilde{F}_4(2), \tilde{E}_7 \tilde{C}_4 \tilde{B}_3, \tilde{C}_{12} \tilde{C}_2, \tilde{D}_8 \tilde{C}_4 \tilde{C}_2, \tilde{A}_{11} \tilde{A}_2(2) \tilde{A}_1(2), \tilde{E}_7 \tilde{C}_6 \tilde{A}_1, \tilde{C}_8 \tilde{C}_6, \tilde{D}_6^2 \tilde{C}_2.$

3H.  $(18, 4, 0)$ . This lattice is isomorphic to

$$U \oplus C_8^2 = U \oplus D_8^2.$$

The Coxeter diagram contains 48 roots. The starting graph is  $G = K_{4,4}$ , the complete bipartite graph on 8 vertices, shown in Figure 5.

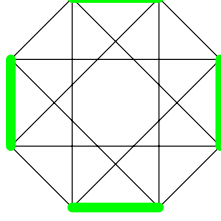


FIGURE 5. Additional roots for  $(18, 4, 0)$

As in Definition 1.3, the subdiagram of the main roots is  $K_{4,4}^{(2)}$ . It has 8  $(-2)$ -roots corresponding to the vertices of  $K_{4,4}$  and 16  $(-2)$ -roots corresponding to the edges of  $K_{4,4}$ , for a total of 24 main roots.

The additional 24  $(-4)$ -roots  $\alpha_C$  are in bijection with the sets of four disjoint edges in  $G$ , i.e. with the perfect matchings on the set of vertices of  $G$ . The intersection numbers are  $\alpha_C \cdot \alpha_{C'} = 4 - 2|C \cap C'|$ . Thus,  $\alpha_C$  and  $\alpha_{C'}$  are connected by a bold line if they don't share any edges, and by a single line if they share exactly one edge.

The graph  $K_{4,4}$  is bipartite, its vertices are split into two groups of four. Denote by  $v^{(1)}$ , resp.  $v^{(2)}$ , the sum of the main roots in the first, resp. the second group. Denote by  $e$  the sum of the main roots for the 16 edges. Then  $a = \frac{1}{4}(2v^{(1)} + e)$  and  $b = \frac{1}{4}(2v^{(2)} + e)$  are two vectors in  $H$  satisfying  $a^2 = b^2 = 0$ ,  $ab = 4$ . They are also orthogonal to the 16 main  $(-2)$ -roots  $\alpha_{ij}^m$  for the edges, which are mutually orthogonal as well. Together they form a standard basis of the sublattice  $(I_{0,16} \oplus U)(2)$  in  $H$ . Thus,  $H$  can be identified with an  $(\text{Aut } K_{4,4})$  lattice lying between it and its dual  $(I_{0,16} \oplus U)(\frac{1}{2})$ .

With the control vector  $v_0 = a + b$ , Vinberg's algorithm terminates in two steps.

The automorphism group of the diagram is  $\text{Aut } \Gamma_r = \text{Aut } K_{4,4} = S_2 \times (S_4 \times S_4)$ . There are 5244 maximal parabolic subgraphs, 17 modulo  $\text{Aut } \Gamma_r$ :

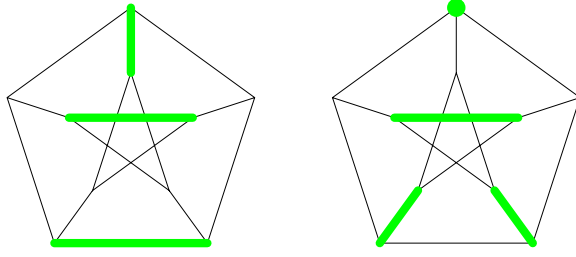
- (1) odd:  $\tilde{D}_8 \tilde{B}_4^2$ ,  $\tilde{E}_8 \tilde{F}_4^2$ ,  $\tilde{E}_7 \tilde{B}_6 \tilde{C}_3(2)$ ,  $\tilde{A}_{11} \tilde{B}_3 \tilde{A}_2(2)$ ,  $\tilde{E}_6^2 \tilde{A}_2^2(2)$ ,  $\tilde{B}_{12} \tilde{F}_4$ ,  $\tilde{D}_6^2 \tilde{C}_2^2(2)$ ,  $\tilde{D}_{10} \tilde{C}_3^2(2)$ ,  $\tilde{B}_8^2$ ,  $\tilde{A}_7^2 \tilde{A}_1^2(2)$ ,  $\tilde{D}_4^3$ .
- (2) even ordinary:  $\tilde{A}_{15} \tilde{A}_1(2)$ ,  $\tilde{E}_7^2 \tilde{C}_2$ ,  $\tilde{D}_{12} \tilde{C}_4$ ,  $\tilde{C}_8 \tilde{E}_8$ ,  $\tilde{C}_{16}$ ,  $\tilde{D}_8^2$ .

3I. **(20, 2, 1)**. This lattice is isomorphic to

$$U \oplus E_8^2 \oplus B_2(2) = U \oplus E_8^2 \oplus A_1^2.$$

The Coxeter diagram was computed by Vinberg and Kaplinskaja in [VK78], see also [Vin83]. For easier comparison with the above diagrams we list the roots in Figure 6. There are 25 main roots for the vertices and edges of the Petersen's graph and 25 additional roots: 20  $(-2)$ -roots of the first kind and 5  $(-4)$ -roots of the second kind.

There are 581 maximal parabolic subdiagrams, 13 modulo  $\text{Aut } \Gamma_r = S_5$ , all odd:  $\tilde{B}_{18}$ ,  $\tilde{B}_{10} \tilde{E}_8$ ,  $\tilde{D}_{16} \tilde{C}_2(2)$ ,  $\tilde{D}_{10} \tilde{E}_7 \tilde{A}_1$ ,  $\tilde{E}_8^2 \tilde{C}_2(2)$ ,  $\tilde{E}_7^2 \tilde{B}_4$ ,  $\tilde{D}_{12} \tilde{B}_6$ ,  $\tilde{D}_8^2 \tilde{C}_2(2)$ ,  $\tilde{A}_9^2$ ,  $\tilde{A}_{15} \tilde{B}_3$ ,  $\tilde{A}_{11} \tilde{E}_6 \tilde{A}_1(2)$ ,  $\tilde{A}_{17} \tilde{A}_1$ ,  $\tilde{D}_6^3$ . On the unique K3 surface with this Picard lattice they

FIGURE 6. Additional roots for  $(20, 2, 1)$ 

define 13 types of elliptic pencils with a section. The rules of Fig. 1 lead to a description of the Kodaira types of the singular fibers in these pencils.

3J. **(15, 9, 1)**. The diagram has 98 roots which modulo  $\text{Aut } \Gamma_r = \text{PSL}(2, 7)$  of order 336 split into four orbits of sizes 14, 14, 14, 56. The first group of 14 forms the subdiagram  $G$  of the main roots. Here,  $G$  is a 4-regular bipartite graph on 14 vertices. It has a natural embedding into the complete bipartite graph  $K_{7,7}$ . The edges of  $G$  in  $K_{7,7}$  are complementary to the edges of the well known Heawood graph, a 3-regular graph on 14 vertices. One way to describe  $G$  is to say that its vertices correspond to the points and lines in the Fano plane  $\mathbb{P}^2$  over  $\mathbb{F}_2$ , and that a line and a point are joined by an edge iff they are *not* incident.

The remaining roots are additional. They are connected to the main roots by 1, 4 and 6 edges. The first of these groups is formed by the  $(-4)$ -roots. This subdiagram is isomorphic to the Heawood graph. Each of these roots is connected to exactly one main root and  $\alpha_i^m \alpha_i = 4$ . The remaining two orbits are formed by the  $(-2)$ -roots of divisibility 2. By [AE22, Lem. 4.14] removing one of these roots and its  $(-2)$ -neighbors gives the Coxeter diagrams for the lattices  $(14, 8, 0)$  and  $(14, 8, 1)$ .

There are 2114 maximal parabolic subdiagrams, and 20 modulo  $\text{Aut } \Gamma_r = \text{Aut } G$ :

- (1) odd:  $\tilde{D}_5 \tilde{B}_3^2 \tilde{A}_1$ ,  $\tilde{A}_7(2) \tilde{A}_3 \tilde{C}_3(2)$ ,  $\tilde{E}_6(2) \tilde{A}_5 \tilde{C}(2)$ ,  $\tilde{C}_6(2) \tilde{B}_4 \tilde{C}_3(2)$ ,  $\tilde{C}_4^3(2) \tilde{A}_1$ ,  $\tilde{E}_7(2) \tilde{B}_5 \tilde{A}_1$ ,  $\tilde{C}_8(2) \tilde{F}_4 \tilde{A}_1$ ,  $\tilde{C}_7(2) \tilde{B}_6$ ,  $\tilde{C}_5(2) \tilde{F}_4^2$ .
- (2) even ord:  $\tilde{A}_7 \tilde{D}_5(2) \tilde{A}_1$ ,  $\tilde{E}_6 \tilde{E}_6(2) \tilde{A}_1$ ,  $\tilde{C}_4^2 \tilde{B}_4(2) \tilde{A}_1$ ,  $\tilde{D}_4 \tilde{B}_3^3(2)$ ,  $\tilde{F}_4^3(2) \tilde{A}_1$ ,  $\tilde{C}_8 \tilde{B}_5(2)$ ,  $\tilde{A}_5 \tilde{A}_5(2) \tilde{C}_3$ ,  $\tilde{E}_7 \tilde{B}_6(2)$ ,  $\tilde{C}_6 \tilde{F}_4(2) \tilde{B}_3(2)$ ,  $\tilde{D}_6 \tilde{B}_5(2) \tilde{C}_2$ ,  $\tilde{C}_6 \tilde{B}_6(2) \tilde{A}_1$ .

3K. **(15, 11, 1)**. There are 66 roots which modulo  $\text{Aut } \Gamma_r = S_2 \times (S_3 \times S_3)$  split into five orbits. The subdiagram of the main roots is the graph  $L(K_{3,3})$ , the line graph of  $K_{3,3}$ , a 4-regular on 9 vertices. The other roots are additional.

The  $(-4)$ -roots are split into two groups of sizes 6, and 9, connected to the main roots by 0, resp. 2 edges. Together, they form the graph  $K_{3,3}^{(2)}$ . There are also two orbits of sizes 6 and 36 connected to the main roots by 3, resp. 5 edges, latter with multiplicities 2, 2, 2, 4, 4. These are  $(-2)$ -roots of divisibility 2. By [AE22, Lem. 4.14] removing one of these roots and its  $(-2)$ -neighbors gives the Coxeter diagrams for the lattices  $(14, 10, 0)$  and  $(14, 10, 1)$ .

There are 522 maximal parabolic subdiagrams, 16 modulo  $\text{Aut } \Gamma_r = \text{Aut } G$ :

- (1) odd:  $\tilde{A}_{11}(2) \tilde{A}_2$ ,  $\tilde{E}_7(2) \tilde{C}_3(2) \tilde{B}_3$ ,  $\tilde{C}_{12}(2) \tilde{A}_1$ ,  $\tilde{E}_8(2) \tilde{F}_4 \tilde{A}_1$ ,  $\tilde{C}_8(2) \tilde{C}_5(2)$ ,  $\tilde{C}_9(2) \tilde{F}_4$ ,  $\tilde{D}_8 \tilde{C}_4(2) \tilde{A}_1$ .

- (2) even ord:  $\tilde{E}_6(2)\tilde{A}_5\tilde{C}_2(2)$ ,  $\tilde{B}_6(2)\tilde{C}_4\tilde{B}_3(2)$ ,  $\tilde{A}_7(2)\tilde{B}_3(2)\tilde{A}_3$ ,  $\tilde{B}_7\tilde{C}_6$ ,  $\tilde{B}_4^3(2)\tilde{A}_1$ ,  
 $\tilde{D}_6(2)\tilde{C}_3^2\tilde{A}_1$ ,  $\tilde{B}_8(2)\tilde{F}_4(2)\tilde{A}_1$ ,  $\tilde{E}_7(2)\tilde{C}_5\tilde{A}_1$ ,  $\tilde{B}_5(2)\tilde{F}_4^2(2)$ .

3L. **(16, 12, 1)**. There are 118 roots which modulo  $\text{Aut } \Gamma_r = S_6$  split into five orbits of sizes 15, 15, 6, 10, 72 of vectors with square  $-2, -4, -4, -2, -4$ . There are 15 main roots forming  $L(K_6)$ , the line graph of the complete graph  $K_6$ .

There are 8917 maximal parabolic subdiagrams, 28 modulo  $\text{Aut } \Gamma_r = \text{Aut } G$ :

- (1) odd:  $\tilde{D}_6^2(2)\tilde{C}_2(2)$ ,  $\tilde{D}_8(2)\tilde{C}_4(2)\tilde{C}_2$ ,  $\tilde{A}_{11}\tilde{A}_2\tilde{A}_1$ ,  $\tilde{C}_8(2)\tilde{C}_6(2)$ ,  $\tilde{C}_{12}(2)\tilde{C}_2(2)$ ,  
 $\tilde{E}_7(2)\tilde{C}_4(2)\tilde{B}_3$ ,  $\tilde{E}_7(2)\tilde{C}_6(2)\tilde{A}_1(2)$ ,  $\tilde{E}_8(2)\tilde{F}_4\tilde{C}_2(2)$ ,  $\tilde{C}_{10}\tilde{F}_4$ ,  $\tilde{D}_{10}(2)\tilde{B}_3\tilde{A}_1(2)$ ,  
(2) even ordinary:  $\tilde{D}_4^2(2)\tilde{C}_3^3(2)$ ,  $\tilde{B}_4^3(2)\tilde{C}_2$ ,  $\tilde{E}_6(2)\tilde{A}_5\tilde{B}_3(2)$ ,  $\tilde{A}_9(2)\tilde{A}_4\tilde{A}_1(2)$ ,  
 $\tilde{D}_6(2)\tilde{C}_3^2\tilde{C}_2$ ,  $\tilde{B}_6(2)\tilde{F}_4^2(2)$ ,  $\tilde{B}_8(2)\tilde{C}_6$ ,  $\tilde{B}_8(2)\tilde{F}_4(2)\tilde{C}_2$ ,  $\tilde{D}_6(2)\tilde{B}_4(2)\tilde{C}_3\tilde{A}_1(2)$ ,  
 $\tilde{A}_7(2)\tilde{A}_3\tilde{B}_3(2)\tilde{A}_1$ ,  $\tilde{E}_8(2)\tilde{C}_6$ ,  $\tilde{E}_7(2)\tilde{C}_5\tilde{C}_2$ ,  $\tilde{A}_5^2(2)\tilde{A}_2^2$ ,  $\tilde{D}_8(2)\tilde{C}_4\tilde{C}_2$ ,  $\tilde{E}_7(2)\tilde{F}_4(2)\tilde{C}_3$ ,  
 $\tilde{B}_{10}(2)\tilde{C}_4$ ,  $\tilde{B}_6^2(2)\tilde{C}_2$ ,  $\tilde{B}_6(2)\tilde{B}_4(2)\tilde{C}_4$ .

**Remark 3.1.** By [AE22, Lem. 5.9], one consequence of listing maximal parabolic subdiagrams in a hyperbolic diagram  $(r, a, 1)$  is the classification of the negative definite even 2-elementary lattices with the invariants  $(r - 2, a, 1)$ ,  $(r - 2, a - 2, 1)$  and  $(r - 2, a - 2, 0)$ .

#### 4. INFINITE AUTOMORPHISM GROUPS OF K3 SURFACES

The main application of the Coxeter diagrams in [Vin83] was the description, for the very first time, of two infinite automorphism groups of K3 surfaces. In the same way our computations imply such a description in several more cases.

A K3 surface  $X$  whose Picard lattice  $S_X$  is 2-elementary comes with a canonical nonsymplectic involution  $\iota$  on  $X$ , acting as  $+1$  on  $S$  and as  $-1$  on the lattice of transcendental cycles  $T = S^\perp$  in  $L_{K3}$ . Any automorphism of  $g$  commutes with  $\iota$ . Let  $Y = X/\iota$  be the quotient surface. It is a rational surface unless  $S = (10, 0, 0)$  in which case  $Y$  is an Enriques surface. Let  $B$  be the branch divisor of  $\pi: X \rightarrow Y$  and denote by  $\text{Aut}'(Y, B)$  the subgroup of  $\text{Aut}(Y, B)$  acting trivially on  $\text{Pic } Y$ .

**Lemma 4.1.** *Let  $S$  be a 2-elementary K3 lattice  $S \neq (10, 10, 0)$ ,  $\Gamma_r$  the Coxeter diagram of  $S$ , and let  $X$  be a K3 surface with Picard lattice  $S_X = S$ . Then there exists an exact sequence*

$$0 \rightarrow \langle \iota \rangle \times \text{Aut}'(Y, B) \rightarrow \text{Aut } X \rightarrow \text{Sym } \Gamma_r \times W(\Gamma_4) \rightarrow 0,$$

where  $\Gamma_4 \subset \Gamma_r$  is the subdiagram formed by the  $(-4)$ -roots, and  $W(\Gamma_4)$  is the corresponding Coxeter group.

*Proof.* A well-known application of Torelli theorem [PSS71] says that for a projective K3 surface with an ample cone  $A(X)$  the natural homomorphism

$$\rho: \text{Aut } X \rightarrow \text{Aut } A(X) = O^+(S)/W_2(S) = O(S)/\pm W_2(S),$$

has finite kernel and cokernel. The kernel of  $\rho$  consists of automorphisms that act trivially on  $S_X$ . They descend to automorphisms of the pair  $(Y, B)$ , and  $\iota$  is the only one descending to the identity. Vice versa, an automorphism of  $(Y, B)$  lifts to an automorphism of  $X$  since  $X = \text{Spec } \mathcal{O} \oplus L^{-1}$  with  $L^2 \simeq \mathcal{O}(B)$  and  $\text{Pic } Y$  has no 2-torsion.  $(\text{Pic } Y) \otimes \mathbb{Q}$  is identified with  $(\text{Pic } X)^\iota \otimes \mathbb{Q} = S \otimes \mathbb{Q}$ . So, the automorphisms of  $X$  acting trivially on  $S$  descend to  $\text{Aut}'(Y, D)$ . Thus,  $\ker \rho = \mathbb{Z}_2 \times \text{Aut}(Y, B)$ .

The homomorphism  $\rho$  is surjective. Indeed, an isometry of  $L_{K3}$  is equivalent to a pair of isometries of  $S$  and  $T$  which have the same image in the finite isometry

group of the discriminant group under  $O(S) \rightarrow O(A_S, q_S) = O(A_T, q_T) \leftarrow O(T)$ . By [Nik79] for an indefinite 2-elementary lattice  $H$ , such as  $S$  and  $T$ , the homomorphism  $O(H) \rightarrow O(A_H, q_H)$  is surjective. So any element of  $O(S)$  can be lifted to  $a \in O(L_{K3})$ . Then a composition  $w \circ a$  with some  $w \in W_2(S)$  sends the fundamental domain  $A(X)$  to itself and therefore is induced by some  $g \in \text{Aut } X$ .

By [Vin83, Prop., p.2] or [AN06, Prop. 2.4] the quotient group  $W(\Gamma_r)/W_2(S)$  is isomorphic to  $W(\Gamma_4)$ . Together with the equality  $O^+(S) = \text{Sym } \Gamma_r \rtimes W(\Gamma_r)$  this gives  $O^+(S)/W_2(S) = \text{Sym } \Gamma_r \rtimes W(\Gamma_4)$ .  $\square$

By [AE22, Sec. 3], for the 2-elementary K3 lattices on the  $g = 1$  line the groups  $\text{Sym } \Gamma_r \rtimes W(\Gamma_4)$  are extensions of affine groups  $W(\tilde{E}_n)$  by dihedral groups. The diagrams of this paper provide even more interesting examples. The  $(-4)$ -subdiagrams for the K3 lattices with  $g = 0$  were given in the previous section. For clarity, we list them in Table 1.  $T_{p,q,r}$  denotes a tree with legs of lengths  $p, q, r$ .

Lattice	$\text{Aut } \Gamma_r$	$\Gamma_4$
(11, 11, 1)	1	$T_{2,3,7}$
(12, 10, 1)	1	$T_{2,4,6} \sqcup A_1$
(13, 9, 1)	$S_3$	$T_{4,4,4}$
(14, 8, 1)	$S_4$	a 10-vertex trivalent tree with 6 ends
(15, 7, 1)	$S_5$	the Petersen graph
(16, 6, 1)	$S_6$	a diagram with 10 + 15 vertices
(18, 4, 0)	$S_2 \times (S_4 \times S_4)$	a diagram with 24 vertices
(20, 2, 1)	$S_5$	$K_5$ with bold edges

TABLE 1. Coxeter diagrams  $\Gamma_4$  defining  $\text{Aut } X$

The diagrams  $\Gamma_4$  for (16, 6, 1) and (18, 4, 0) are quite complicated, and have both simple and bold edges. It is a little easier to describe the subdiagram  $\Gamma'_4$  of  $\Gamma_4$  with the bold edges removed. The Coxeter group  $W(\Gamma'_4)$  is the quotient of  $W(\Gamma_4)$  by the additional commuting relations for the bold edges.

For (16, 6, 1) the graph  $\Gamma'_4$  is a union of 10 disjoint vertices and  $L(K_6)$ .

For (18, 4, 0) the graph  $\Gamma'_4$  is a union of two disjoint subgraphs  $G_1 \sqcup G_2$ , and each  $G_i$  can be defined as the complement of  $K_4 \sqcup K_4 \sqcup K_4$  in the complete graph  $K_{12}$ . This means that an edge of  $K_{12}$  is in  $G_i$  iff it is not in  $K_4 \sqcup K_4 \sqcup K_4$ .  $G_i$  is an 8-regular graph on 12 vertices.

## REFERENCES

- [AE22] Valery Alexeev and Philip Engel, *Mirror symmetric compactifications of moduli spaces of K3 surfaces with a nonsymplectic involution*, [arXiv:2208.10383](https://arxiv.org/abs/2208.10383) (2022).
- [AN06] Valery Alexeev and Viacheslav V. Nikulin, *Del Pezzo and K3 surfaces*, MSJ Memoirs, vol. 15, Mathematical Society of Japan, Tokyo, 2006, [arXiv:math/0406536](https://arxiv.org/abs/math/0406536).
- [Nik79] V. V. Nikulin, *Integer symmetric bilinear forms and some of their geometric applications*, *Izv. Akad. Nauk SSSR Ser. Mat.* **43** (1979), no. 1, 111–177, 238.
- [Nik81] ———, *Quotient-groups of groups of automorphisms of hyperbolic forms by subgroups generated by 2-reflections. Algebro-geometric applications*, Current problems in mathematics, Vol. 18, Akad. Nauk SSSR, Vsesoyuz. Inst. Nauchn. i Tekhn. Informatsii, Moscow, 1981, pp. 3–114.
- [PSS71] I. I. Pjateckiĭ-Shapiro and I. R. Shafarevič, *Torelli's theorem for algebraic surfaces of type K3*, *Izv. Akad. Nauk SSSR Ser. Mat.* **35** (1971), 530–572.

- [Sag22] Sage Developers, *Sagemath, the Sage Mathematics Software System (Version 9.5)*, 2022, <https://www.sagemath.org>.
- [Vin72] È. B. Vinberg, *The groups of units of certain quadratic forms*, Mat. Sb. (N.S.) **87(129)** (1972), 18–36.
- [Vin75] ———, *Some arithmetical discrete groups in Lobačevskii spaces*, Discrete subgroups of Lie groups and applications to moduli (Internat. Colloq., Bombay, 1973), Oxford Univ. Press, Bombay, 1975, pp. 323–348.
- [Vin83] ———, *The two most algebraic K3 surfaces*, Math. Ann. **265** (1983), no. 1, 1–21.
- [VK78] È. B. Vinberg and I. M. Kaplinskaja, *The groups  $O_{18,1}(Z)$  and  $O_{19,1}(Z)$* , Dokl. Akad. Nauk SSSR **238** (1978), no. 6, 1273–1275.

*Email address:* [valery@uga.edu](mailto:valery@uga.edu)

DEPARTMENT OF MATHEMATICS, UNIVERSITY OF GEORGIA, ATHENS GA 30602, USA